

Synthetic Dataset Generation for Privacy-Preserving Machine Learning

Efstathia Soufleri, Gobinda Saha, and Kaushik Roy

Abstract—Machine Learning (ML) has achieved enormous success in solving a variety of problems in computer vision, speech recognition, object detection, to name a few. The principal reason for this success is the availability of huge datasets for training deep neural networks (DNNs). However, datasets cannot be publicly released if they contain sensitive information such as medical records, and data privacy becomes a major concern. Encryption methods could be a possible solution, however their deployment on ML applications seriously impacts classification accuracy and results in substantial computational overhead. Alternatively, obfuscation techniques could be used, but maintaining a good trade-off between visual privacy and accuracy is challenging. In this paper, we propose a method to generate secure synthetic datasets from the original private datasets. Given a network with Batch Normalization (BN) layers pretrained on the original dataset, we first record the class-wise BN layer statistics. Next, we generate the synthetic dataset by optimizing random noise such that the synthetic data match the layer-wise statistical distribution of original images. We evaluate our method on image classification datasets (CIFAR10, ImageNet) and show that synthetic data can be used in place of the original CIFAR10/ImageNet data for training networks from scratch, producing comparable classification performance. Further, to analyze visual privacy provided by our method, we use Image Quality Metrics and show high degree of visual dissimilarity between the original and synthetic images. Moreover, we show that our proposed method preserves data-privacy under various privacy-leakage attacks including Gradient Matching Attack, Model Memorization Attack, and GAN-based Attack.

Index Terms—Synthetic Images, Privacy, Deep Learning, Neural Networks, Privacy-Preserving Machine Learning

I. INTRODUCTION

MACHINE Learning (ML) has been integrated with great success in a wide range of applications such as computer vision, autonomous driving, speech recognition, natural language processing, object detection and so on. The availability of large datasets and advancements in techniques

This work was supported in part by the Center for Brain Inspired Computing (C-BRIC), one of the six centers in Joint University Microelectronics Program (JUMP), in part by the Semiconductor Research Corporation (SRC) Program sponsored by Defense Advanced Research Projects Agency (DARPA), in part by the Semiconductor Research Corporation, in part by the National Science Foundation; in part by the Department of Defense (DoD) Vannevar Bush Fellowship, in part by the U.S. Army Research Laboratory, and in part by IARPA.

Efstathia Soufleri is with School of Electrical and Computer Engineering, Purdue University, West Lafayette, IN 47907, USA (e-mail: esoufler@purdue.edu).

Gobinda Saha is with School of Electrical and Computer Engineering, Purdue University, West Lafayette, IN 47907, USA (e-mail: gsaha@purdue.edu).

Kaushik Roy is with School of Electrical and Computer Engineering, Purdue University, West Lafayette, IN 47907, USA (e-mail: kaushik@purdue.edu).

(Under Submission)

for training deep neural network models have played integral roles towards such success. Moreover, the cloud providers offer various Machine Learning as a Service (MLaaS) platforms such as Microsoft Azure ML Studio [1], Google Cloud ML Engine [2], and Amazon Sagemaker [3] etc., where computational resources is provided for running ML workloads. For such cloud-based computing, the ML algorithms are either provided by the users or selected from the standard ML algorithm libraries [4], whereas the datasets are usually shared to cloud by the users to meet application-specific requirements. However, it might not be always possible to share private data to the cloud if they contain sensitive information such as medical or financial records or the user may need to follow certain terms and regulations that forbid public release of the data.

Thus, it is essential to protect the privacy of the training data before publicly releasing them, as this would offer numerous advantages. First, it will be beneficial for the research community - scientists could open source their data without privacy concerns and consequences. Access to the data will facilitate researchers to reproduce experiments from other studies and hence, transparency will be promoted. Additionally, by combining data from different sources can lead to better models that can be built. Moreover, data can potentially be traded in data markets, where protection of sensitive information is of utmost importance [5]. Overall, collaboration between users will be facilitated and this will help in a broader way towards advancements in ML research.

In literature, several proposals have been suggested to ensure visual privacy of the data. Among those methods, a popular approach is data encryption [6], [7], [8], [9], [10], [11], where the user encrypts the data before sending to the cloud. This is considered to be a highly successful method and has demonstrated exceptional results for protecting the data privacy [12], [13]. However, this method is computationally expensive making it prohibitive for wide adaptation in ML applications [14]. Alternatively, researchers have suggested several image-obfuscation techniques for visual privacy preservation [5]. These techniques include image blurring [15], mixing [16], [17], adding noise [4], pixelizing [18] etc., which allow the model to be trained with the obfuscated images and achieve good accuracy-privacy trade-off. However, when the images are highly obfuscated, though visual privacy is well ensured, the performance of the network might drop beyond the desirable point.

In this paper, we introduce an algorithm for generating secure synthetic data from the original private data. Specifically, as inputs, our method requires the original data and a network

with Batch Normalization (BN) layers pre-trained on these data. For each class in the original dataset, we fine-tune the pre-trained network on a subset of samples ($\sim 25\%$ of the total training samples) of the corresponding class and record the BN statistics - the running mean and running variance - from each layer. Then, we initialize the synthetic data as Gaussian noise and optimize them to match the recorded BN statistics [19]. Upon generation of the synthetic dataset, they can be publicly released and used for training DNNs from scratch. We evaluate our methodology on widely used image classification datasets - CIFAR10 [20] and ImageNet [21]. We test whether the synthetic data generated from our method satisfy two important properties: i) data-utility, and ii) privacy-preservation. The data-utility property implies that when the original data are replaced by synthetic data, the ML application maintains performance. We examined, if a network when trained with synthetic data, is able to converge and maintain the classification accuracy compared to the same network trained on the original data. The experimental evaluation reveals that the synthetic data generated with our proposed method maintain this property. Moreover, it is important to ensure that the synthetic data do not leak substantial visual information about the original data - privacy-preservation property. To verify that, we compare the synthetic images with the original images using the following Image Quality Metrics (IQMs) [18]: Mean-Square-Error (MSE) [22], Structural Similarity Index Measure (SSIM) [23], and Haar wavelet-based perceptual similarity index (HaarPSI) [24]. Analyses of the metrics show that there is high degree of visual dissimilarity between the original images and the synthetic images obtained from our method. However, visual dissimilarity may not necessarily imply that the synthetic images won't leak sensitive information about the original dataset. Therefore, to complement the image quality analysis, we further perform the privacy-leakage attacks such as Gradient Matching Attack [25], Model Memorization Attack [26], and GAN-based Attack [27]. These attacks aim to reconstruct the original images of the training dataset. In our experiments we observe that when the synthetic dataset and (or) a network trained on this dataset is available, the attacker might recover the synthetic data, but the attacker is not able to leak further visual information about the original dataset. Overall, the results provide strong evidences for the effectiveness of our method in generating secure and synthetic datasets for privacy preserving ML applications.

Our main contributions are summarized as following:

- To facilitate privacy-preserving ML applications, we propose a new method for generating synthetic data based on the original dataset and the BN statistics of a neural network pre-trained on it.
- With detailed analysis, we show that the generated synthetic dataset has both data-utility and privacy-preservation properties.
- Our experiments on image classification datasets including CIFAR10 and ImageNet verify the utility of the synthetic dataset. Moreover, we verify the visual privacy of the dataset using Image Quality Metrics (IQM) along with Gradient Matching Attack [25], Model Memoriza-

tion Attack [26], and GAN-based Attack [27].

The rest of the paper is organized as follows: in Section II we discuss the related works and in Section III we describe our proposed method. In Section IV, we evaluate our method on image classification datasets and analyze the data-privacy and privacy-preservation properties. Finally, in Section V we conclude the paper with future research perspectives.

II. RELATED WORK

A. Data Privacy in Machine Learning

One approach to tackle the problem of maintaining data privacy is to apply noise on the input or the gradients of the NN in a differentially private manner [28], [29], [30], [31]. Differentially Private Stochastic Gradient Descent (DPSGD) [32] method clips and adds noise in the gradients of the model during training in order to prevent the model to leak information regarding the data. Authors in [33], [34] apply noise directly to the raw input data. The above approaches provide strong privacy guarantees at the detriment of accuracy.

Image obfuscation is a technique that visually distorts parts or the entire image [4], [35], [18], [5], [36], [37]. Thus, they are able to hide the sensitive information and securely release the images for ML applications. Zhang et al. [4] add noise in the image, train an NN and then evaluate it against model inversion attack [38], model classification attacks [39], membership inference attack [40] and model memorization attack [26]. Authors in [18] apply blurring, pixelization and other forms of distortion on the image. They perform a study that evaluates which metrics are aligned with human perception as well as how much distortion is required such that the image can not be classified correctly. They evaluate various image quality metrics and conclude that Structural Similarity Index Measure (SSIM) and Haar wavelet-based perceptual similarity index (HaarPSI) align better with the human perception [18]. Authors in [41] generate proxy data deployed in order to encode gradient updates during NN training in a federated learning set-up. They propose using cross entropy loss with per example weighted average. This weighted loss is optimized to align the gradient from the synthetic data with the real data. Additionally, to capture scale information they send scaling values for each layer to the synthetic update. Researchers in [5] present a method for generating Differential Private (DP) synthetic data. This method adds noise in the data generated by a Generative Adversarial Network (GAN). However, the images might reveal information about the original images or might not maintain the utility of the data resulting in high accuracy degradation.

Another direction is the privacy-preserving data release [5], [34], [42], [43]. This approach offers numerous advantages such as any model can be trained flexibly on the released data, combined data from different sources can be used to build stronger models etc. Our proposal falls in this category. We suggest a method for generating the synthetic images that preserves the statistical properties of the original images, without revealing visual information that can be used to backtrack the original images. Note, that our proposed method can potentially be used in conjunction with the aforementioned

DPSGD method, adding one more layer of protection against attacks.

B. Synthetic Image Generation in other ML Applications

In the literature, there are works that propose to synthesize fake images using the BN statistics (mean and variance) of a pretrained network. ZeroQ [19] generates synthetic data using such statistics for quantizing weights and activations of an NN without accessing the original training dataset. For data generation, ZeroQ does not consider the cross-entropy loss and uses the BN statistics corresponding to all the classes of the dataset. Similarly, IntraQ [44] generates synthetic images using BN statistics along with local object reinforcement, marginal distance constraint, and soft inception loss to improve the performance of zero-shot network quantization. Moreover, authors in [45], [46] utilize the BN statistics combined with additional losses (e.g. inception loss, adversarial loss) to synthesize fake images for fine-tuning model during quantization. Our work, on the other hand, collects BN statistics for each class individually and includes cross-entropy loss in the total loss function, since we aim the generated images of different classes to have heterogeneous features to preserve data-utility.

Furthermore, there is emerging research that focuses on generating realistically looking images for data-free ML applications [47] such as data-free pruning, data-free incremental learning [48] and data-free network knowledge distillation [49]. For instance, Deep Inversion [50] aim to generate real-looking images without sharp transitions in the adjacent pixels. The loss function that they use is similar to ours, but they use additional terms and coefficients in order to guarantee that the generated images look natural. Moreover, GZNQ [51] synthesizes realistic images from a generative model using BN statistics for data-free model quantization. In contrast, our work aims to generate images that have high degree of visual dissimilarity to the natural images to ensure visual privacy. Moreover, unlike these prior works, we analyze the data-utility and transferability of the generated synthetic dataset when training networks from scratch. In addition, we provide a systematic framework for analyzing their visual privacy using various IQMs and privacy-leakage attacks for enabling privacy-preserving ML applications.

III. METHOD

In this section, first we describe our algorithm for generating synthetic images from original dataset. Then, we discuss the two important properties for the synthetic images that enable privacy-preserving ML.

A. Synthetic Image Generation

In this section, we describe the methodology for generating the synthetic data. Figure 1 gives an overview of the proposal. A neural network (NN) with BN layers is first trained on the original images. Then, for each class of the original images, the NN is fine-tuned on the images of the class. The images of each class affect the BN statistics, namely the mean (μ) and the variance (σ), in a different way. As we generate the

Algorithm 1 : Synthetic Image Generation

- 1: **Require:** Original Images, NN with L BN layers pre-trained on the original images
 - 2: **Output:** Synthetic Images
 - 3: Let C be the number of classes of the original dataset
 - 4: Let $iter$ be the number of iterations for synthetic image generation
 - 5: **Generation of Synthetic Images:**
 - 6: **for** $i = 1, 2, \dots, C$ **do**
 - 7: Fine-tune the NN on a subset of original images (x)
 - 8: Record the BN statistics (μ, σ)
 - 9: Generate random data x^s from Gaussian Noise
 - 10: **for** $j = 1, 2, \dots, iter$ **do**
 - 11: Forward Propagation $NN(x^s)$
 - 12: Record the running BN statistics ($\tilde{\mu}_i^s, \tilde{\sigma}_i^s$)
 - 13: Compute the loss from eq. 1
 - 14: Backward Propagation
 - 15: Update x^s
 - 16: **end for**
 - 17: Synthetic Images = Synthetic Images $\cup x^s$
 - 18: **end for**
 - 19: **Return** Synthetic Images of all the classes
-

synthetic images class-wise, we record the statistics of each class - not the entire dataset. Initially, we define the synthetic images of the corresponding class as random Gaussian noise. These images are optimized based on a loss function such that it resembles the statistics of the corresponding class of the original dataset. To generate synthetic images (x^s), we optimize the following loss function:

$$\min_{x^s} \sum_{n=1}^L \|\tilde{\mu}_i^s - \mu_i\|_2^2 + \|\tilde{\sigma}_i^s - \sigma_i\|_2^2 + f(labels, NN(x^s)) \quad (1)$$

where μ_i and σ_i are the mean and variance at layer i of the NN recorded based on the original images (x), whereas $\tilde{\mu}_i^s$ and $\tilde{\sigma}_i^s$ are the running mean and running variance of the synthetic images (x^s) at layer i . L is the number of layers of the pre-trained network, $NN(x^s)$ is the output of the NN when x^s is fed as an input, and f denotes the cross-entropy loss between the actual labels and the output of the network. Essentially, this optimization process aims to generate class-wise synthetic images (x^s) such that, when fed in the NN, produces layer-wise statistical distributions that closely matches distributions of the original images. The synthetic images obtained after such optimization steps can be released publicly to enable privacy-preserving ML applications. The steps for generating these images in the form of pseudo-code is given in Algorithm 1.

B. Synthetic Image Properties

The synthetic images should satisfy the following two properties: (i) data-utility preservation and (ii) privacy-preservation.

Data-utility implies that the original images can be replaced by the synthetic without affecting the performance of the

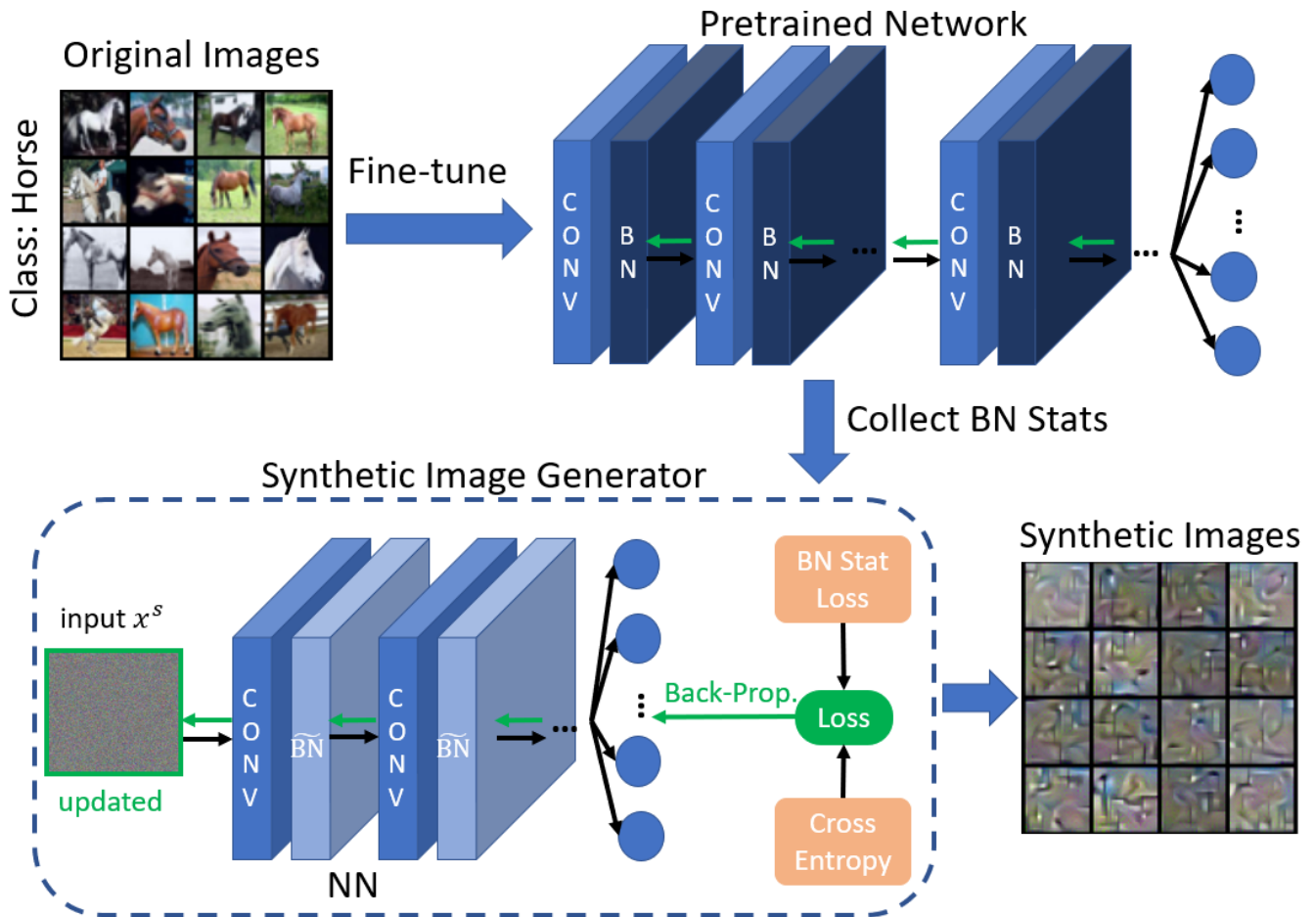


Fig. 1. Overview of the proposed method. The pretrained network is fine-tuned class-wise and the BN statistics (mean, variance) are collected. The Synthetic Image Generator optimizes random noise such that the synthetic images have a statistical distribution that closely matches the original data on the pretrained NN. The BN stat loss is: $\sum_{n=1}^L \|\mu_i^{s^*} - \mu_i\|_2^2 + \|\sigma_i^{s^*} - \sigma_i\|_2^2$ between the collected BN statistics (μ_i, σ_i) and the running mean and variance $(\mu_i^{s^*}, \sigma_i^{s^*})$ of the synthetic images (x^s) and the cross entropy loss is: $f(\text{labels}, NN(x^s))$ between the actual label and the output of the NN on synthetic data.

ML application. This is of utmost importance because the accuracy of the NN should not degrade beyond an acceptable point. In our work, we test the utility of the synthetic dataset by first training a NN from scratch with original images. Then, training an NN with same network architecture from scratch with synthetic images. Similar accuracy in both cases would mean that the synthetic data have high utility. As it is later demonstrated in the experiment section, our synthetic images satisfy this property. Moreover, we show that data-utility property transfers across different network architectures.

Privacy-preservation appears to be more difficult concept to quantify. An initial step to evaluate this property is using the visual dissimilarity between the synthetic and the original images. Such dissimilarity is quantified by the following Image Quality Metrics (IQMs) [18]: Mean-Square-Error (MSE), Structural Similarity Index Measure (SSIM), and Haar wavelet-based perceptual similarity index (HaarPSI). The MSE [22] is the squared pixel-wise distance between the synthetic and the original image. It is not upper bounded and higher value denotes higher dissimilarity. SSIM [23] is used for determining the perceived quality of the synthetic images

based on the original images as a reference. SSIM measures the spatial correlation consisting of three components: mean, variance, and cross-correlation. Its values vary in $[0, 1]$ range, where values close to zero denote highly dissimilar images and values equal to one denotes images perfectly matched. HaarPSI [24] uses the coefficients obtained from a Haar wavelet decomposition to assess local similarities between two images. Here, values near zero denote dissimilarity. According to [18], SSIM and HaarPSI are the two metrics that closely resemble human perception. Therefore, in our study we evaluate all the aforementioned metrics but we emphasize more on these two metric to verify whether the synthetic images maintain visual features from the original images. Later, in the experiment section, we show that the synthetic images from our method do not acquire visual features similar to the original images.

However, the visual dissimilarity between the synthetic and the original images may not necessarily imply that the synthetic images will not reveal important information about the original images. Thus, to further verify the privacy of the synthetic images, we perform the following privacy-leakage

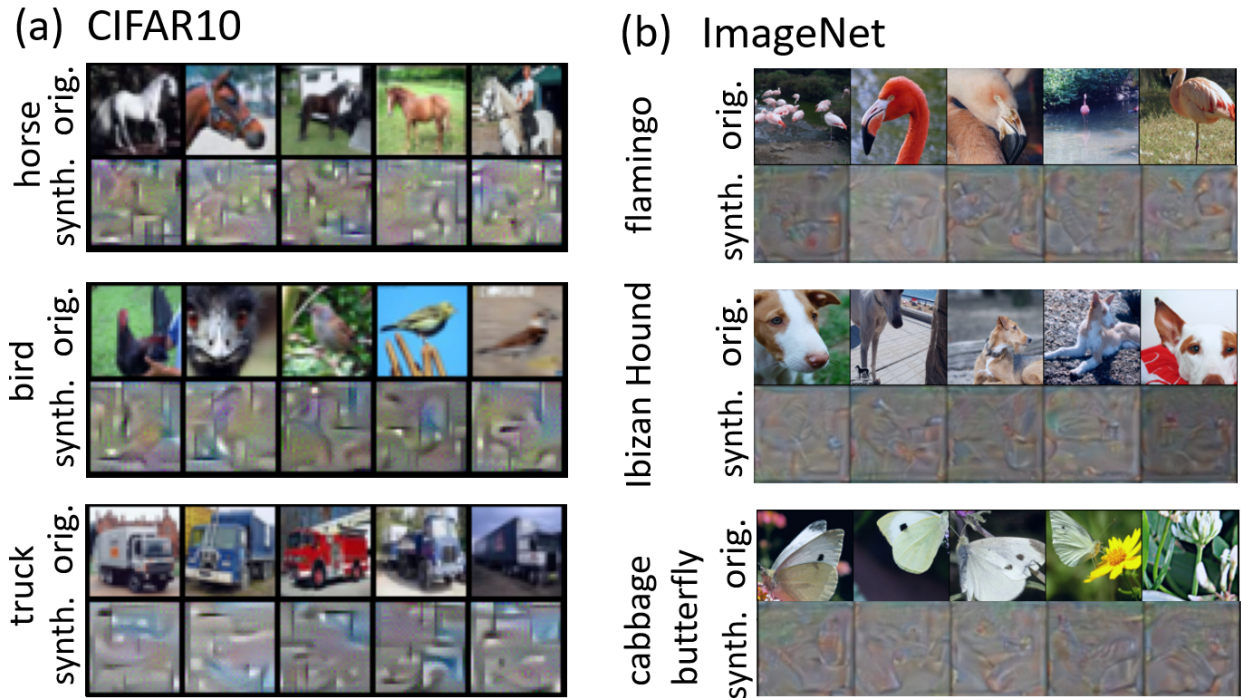


Fig. 2. Example of Original and corresponding Synthetic images of a) CIFAR10 and b) ImageNet. Here synthetic images are generated with our proposed method.

attacks: Gradient Matching Attack [25], Model Memorization Attack [26], and GAN-based Attack [27]. These attacks aim to reconstruct or leak information of the original training images. The **Gradient Matching Attack** shows that it is possible to obtain the training data if the gradients of the model are exposed to the attacker. The authors in [25] demonstrate that starting from random inputs, it is possible to reconstruct the original image by matching the gradients. Indeed, the leakage is pixel-wise accurate for the image. Furthermore, we perform the **Model Memorization Attack** [26], where the attacker is interested in recovering specific sensitive images of the training set. The attacker can steal sensitive samples and encode them in the model parameters or model output. Then, another malicious party can retrieve them when serving the model. Encoding methods include least significant (lower) bits (LSB) of the model parameters, correlated value encoding, and sign encoding. Moreover, we evaluate the robustness of our method against **GAN-based Attack** [27]. This attack aims to reconstruct the images of a specific class during network training using a Generative Adversarial Network (GAN). Specifically, let a be the target class that the attacker desires to reconstruct. The GAN consists of a generator network (G) and a discriminator network (D). The network is trained on the synthetic data. The attack follows the process described below: an instance of the network is copied to D ; run G on D targeting class a ; update G based on the answer from D ; get n samples of class a generated by G ; assign a fake label to the samples and merge them with the dataset. This process is repeated at each training epoch of the network. At the end of the attack, the adversary has n images of class a . The pseudocodes of the Gradient Matching Attack and GAN-based Attack are provided in Algorithm 2 and Algorithm 3, respectively, in

the Appendix. In the experiment section, we show that our method is robust under these attacks as our synthetic images do not leak any visually sensitive information about the original images.

IV. EXPERIMENTS AND RESULTS

A. Experimental Setups

We evaluate our proposed method on popular image classification datasets - CIFAR10 [20] and ImageNet [21]. We use ResNet20 [52] and VGG11-BN [53] models for CIFAR10 and ResNet18 [52] and MobileNetV2 [54] models for ImageNet experiments. Figure 2 illustrates examples of synthetic images of CIFAR10 and ImageNet dataset generated by our method in reference to the original images. We implemented our experiments using the PyTorch framework [55] on a system with a NVIDIA GTX 1080 Ti GPU. For the class-wise fine-tuning on CIFAR10/ImageNet, we use SGD optimizer [56] with 0.01 learning rate and momentum = 0.9 for 5 epochs. We use $\sim 25\%$ of the images of each class during the fine-tuning phase. For generating the synthetic images (CIFAR10/ImageNet), we use Adam optimizer [57] with learning rate = 0.5, $\beta = (0.9, 0.999)$, and batch size = 64 for 250 iterations. For training the models on the synthetic dataset, we use SGD optimizer [56] with learning rate = 0.1 and reduce learning rate by 10 after every 50 epochs. The models are trained for 200 epochs with batch size = 256 for CIFAR10 and for 70 epochs with batch size = 64 for ImageNet. The models pretrained on CIFAR10 and ImageNet were obtained from the pytorch pretrained models [55] or the pytorchcv open source library [58], when available. When a pretrained model was not available (e.g. VGG11-BN), we followed the same training protocol as mentioned above.

TABLE I

CLASSIFICATION RESULTS (TOP-1 ACCURACY) AVERAGED OVER 5 RUNS FOR RESNET20 AND VGG11-BN NETWORKS TRAINED ON SYNTHETIC AND ORIGINAL CIFAR10 IMAGES. THE SYNTHETIC IMAGES WERE GENERATED USING THE BN STATISTICS OF THE CORRESPONDING PRETRAINED RESNET20 AND VGG11-BN NETWORKS ON CIFAR10.

Model	Accuracy	
	Synthetic Images	Original Images
ResNet20	93.32% ± 0.7	94.03% ¹
VGG11-BN	91.12% ± 0.3	92.11% ± 0.4

TABLE II

CLASSIFICATION RESULTS (TOP-1 ACCURACY) AVERAGED OVER 5 RUNS FOR RESNET18 AND MOBILENETV2 NETWORKS TRAINED ON SYNTHETIC AND ORIGINAL IMAGENET IMAGES. THE SYNTHETIC IMAGES WERE GENERATED USING THE BN STATISTICS OF THE CORRESPONDING PRETRAINED RESNET18 AND MOBILENETV2 NETWORKS ON IMAGENET.

Model	Accuracy	
	Synthetic Images	Original Images
ResNet18	67.85% ± 0.5	69.75% ²
MobileNetV2	69.42% ± 1.0	71.87% ²

B. Data Utility

1) *Data Utility of the Synthetic Dataset*: It is desirable that the synthetic images maintain their utility. We verify this property by first reporting the classification accuracy of ResNet20 and VGG11-BN when trained on the original CIFAR10 dataset. Then, we train the networks with the same architecture, i.e. ResNet20 and VGG11-BN from scratch on the synthetic images generated from CIFAR10. Table I summarizes the accuracy for both cases. We observe that the networks trained on original and synthetic images perform similar. There is $\sim 0.7\%$ and $\sim 1\%$ accuracy drop respectively for ResNet20 and VGG11-BN on synthetic images compared to the original images. Next, we perform the same experiment for ImageNet using ResNet18 and MobileNetV2 models. We note that data utility also is preserved in this case with a slightly higher accuracy drop of $\sim 1.9\%$ and $\sim 2.4\%$. Table II summarizes the accuracy results for ImageNet trained on ResNet18 and MobileNetV2 models.

2) *Transferability of the Synthetic Dataset*: In the above experiments, the synthetic images were generated and evaluated using the same network architectures. For instance, the BN statistics (mean, variance) were collected from a ResNet20 model pretrained on CIFAR10 and then the same ResNet20 model was trained from the scratch on synthetic CIFAR10 images and accuracy was tested. Now, we would like to test if the synthetic images generated from a specific network architecture can be successfully used for training other network architectures from scratch or not. To verify this, we perform the following experiment: first, we generate synthetic images using the BN statistics of ResNet20 trained on CIFAR10 and then we train VGG11-BN, ResNet56 and DenseNet40 models from scratch on these synthetic images. We compare the accuracy with the case of training VGG11-BN [53], ResNet56 [52] and DenseNet40 [59] on the original CIFAR10

TABLE III

CLASSIFICATION RESULTS (TOP-1 ACCURACY) AVERAGED OVER 5 RUNS FOR VGG11-BN, RESNET56 AND DENSENET40 NETWORKS TRAINED ON SYNTHETIC AND ORIGINAL CIFAR10 IMAGES. THE SYNTHETIC IMAGES WERE GENERATED USING THE BN STATISTICS OF A PRETRAINED RESNET20 NETWORK ON CIFAR10.

Model	Accuracy	
	Synthetic Images	Original Images
VGG11-BN	91.12% ± 0.3	92.11% ± 0.4
ResNet56	94.30% ± 0.7	95.48% ¹
DenseNet40	93.27% ± 0.3	94.39% ¹

TABLE IV

CLASSIFICATION RESULTS (TOP-1 ACCURACY) AVERAGED OVER 5 RUNS FOR VGG19-BN, RESNET50 AND DENSENET121 NETWORKS TRAINED ON SYNTHETIC AND ORIGINAL IMAGENET IMAGES. THE SYNTHETIC IMAGES WERE GENERATED USING THE BN STATISTICS OF A PRETRAINED RESNET18 NETWORK ON IMAGENET.

Model	Accuracy	
	Synthetic Images	Original Images
VGG19-BN	72.97% ± 0.4	74.24% ²
ResNet50	75.27% ± 0.5	76.15% ²
DenseNet121	73.16% ± 0.4	74.65% ²

images. Table III shows the accuracy comparison. A similar experiment was conducted for ImageNet dataset for training VGG19-BN, ResNet50, and DenseNet121 on synthetic images extracted from a ResNet18 network (Table IV). We observe that the networks perform similar when trained on synthetic and original images. Thus, we believe that the utility of the synthetic images generated by our method using a specific network architecture is transferable and the synthetic data can be successfully used to train other network architectures.

C. Privacy Preservation

1) *Image Quality Metrics (IQM)*: The visual information leak is evaluated using the following metrics: MSE, SSIM, and HaarPSI. Table V contains the MSE, SSIM, and HaarPSI for CIFAR10 and ImageNet. We generate class-wise batches of synthetic images from the BN statistics of the corresponding original images. It is worth noting that, in our method there is no one-to-one correspondence between the synthetic images and the original images. Thus, the evaluation metrics are computed pairwise between the batches of each class of the original and the generated synthetic images. The visual perception is subjective so it is necessary to compare the computed values with a reference. For this purpose, we calculate the visual similarity of a batch of original images and random noise. Based on the image quality metrics from Table V for CIFAR10 and ImageNet, it is evident that there is high degree of visual dissimilarity between the original images and random noise. Whereas, the original and the generated synthetic images are as dissimilar as the original image/random noise dissimilarity reference. Although these metrics provides a reasonable measure for visual dissimilarity, they alone might not be sufficient for providing guarantee that the synthetic images will not leak visual information about the original images. Therefore, in the next sub-section we test the synthetic images under various privacy-leakage attacks.

¹model obtained from open library pytorchcv

²model obtained from pytorch pretrained models

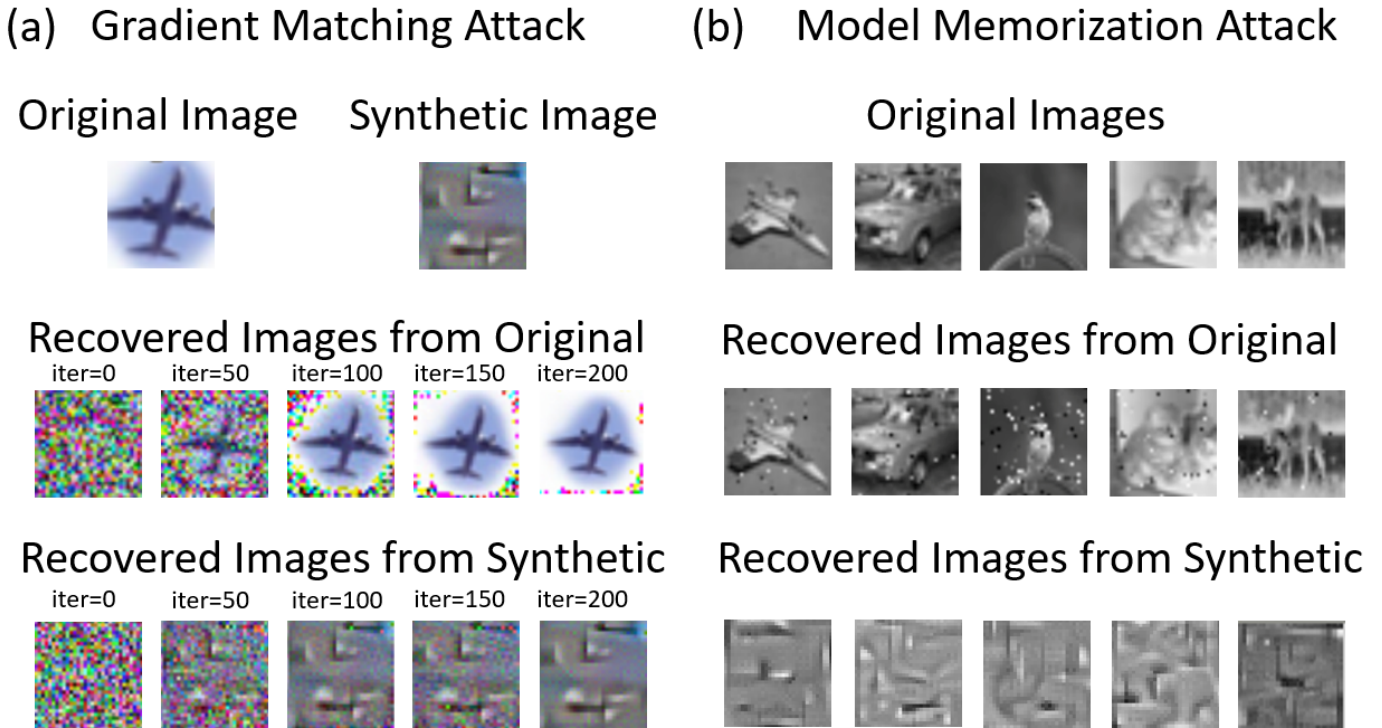


Fig. 3. (a) Gradient Matching Attack: targeting a original image (airplane from CIFAR10), and targeting a synthetic image (airplane). In both cases, the attacker is able to reconstruct with high fidelity the target image. However, for the synthetic images the attacker cannot go beyond that and obtain the original image. (b) Model Memorization Attack on CIFAR10: Original Images, Recovered Images when encoding Original Images in the model and, Recovered Images when encoding Synthetic Images in the model.

TABLE V
EVALUATION USING IMAGE QUALITY METRICS ON CIFAR10 AND IMAGENET. HIGHER MSE, SSIM AND HAARPSI DENOTE HIGHER DISSIMILARITY AMONG DIFFERENT SETS OF IMAGES E.G. ORIGINAL/SYNTHETIC IMAGES AND ORIGINAL IMAGES/RANDOM NOISE.

Dataset	Metric	Original/Synthetic Images	Original Images/Random Noise
CIFAR10	MSE	3.0144	3.0850
	SSIM	0.0100	0.0039
	HaarPSI	0.2731	0.2552
ImageNet	MSE	2.0112	2.1999
	SSIM	0.0018	0.0013
	HaarPSI	0.2632	0.2810

2) *Privacy-leakage Attacks*: We first evaluate the **Gradient Matching Attack** [25]. This attack aims to reconstruct the training data from the publicly shared gradients of the network. Given a original image, we compute its corresponding gradients and feed them as an input to the attack. From Figure 3 (a), we observe that the image is successfully reconstructed at the last iteration by such an attack. Whereas, if a synthetic image is used, the gradient matching attack is able to reconstruct the synthetic image successfully, but cannot obtain the original image. Thus, our experiments suggest that with gradient matching attack it will not be possible to recover the original source images from which synthetic images were generated.

Next, we test our proposal on **Model Memorization Attack** [26]. In this case the adversary could be a malicious cloud provider in a model training service. In this attack, the attacker has full access to the training set and the model. The attacker is interested in some sensitive samples whose values are encoded into the model parameters. Later, another malicious party that

deploys the model can retrieve the sensitive images that the attacker has encoded. We use the attack from Song et al. [26] that encodes 400 images from CIFAR10 dataset into a ResNet34 [52] model. The first row of Figure 3 (b) illustrates the original images encoded in the ResNet34 model. Then, the second row of Figure 3 (b) depicts the recovered original images from the compromised model. Following the attack protocol, the images are converted into gray-scale images for this attack. We observe that the adversary accurately recovers most pixels of the image and the objects are easily identified. Finally, the third row depicts the recovered synthetic images when synthetic images are encoded in the model by the attacker. The recovered images are highly distorted and image details are hard to be recognized. Thus, similar to the gradient matching attack, this attack does not allow original images to be recovered from the synthetic images.

Next, we evaluate our method using the **GAN-based attack** [27] described in Section III-B. For this method, attacker

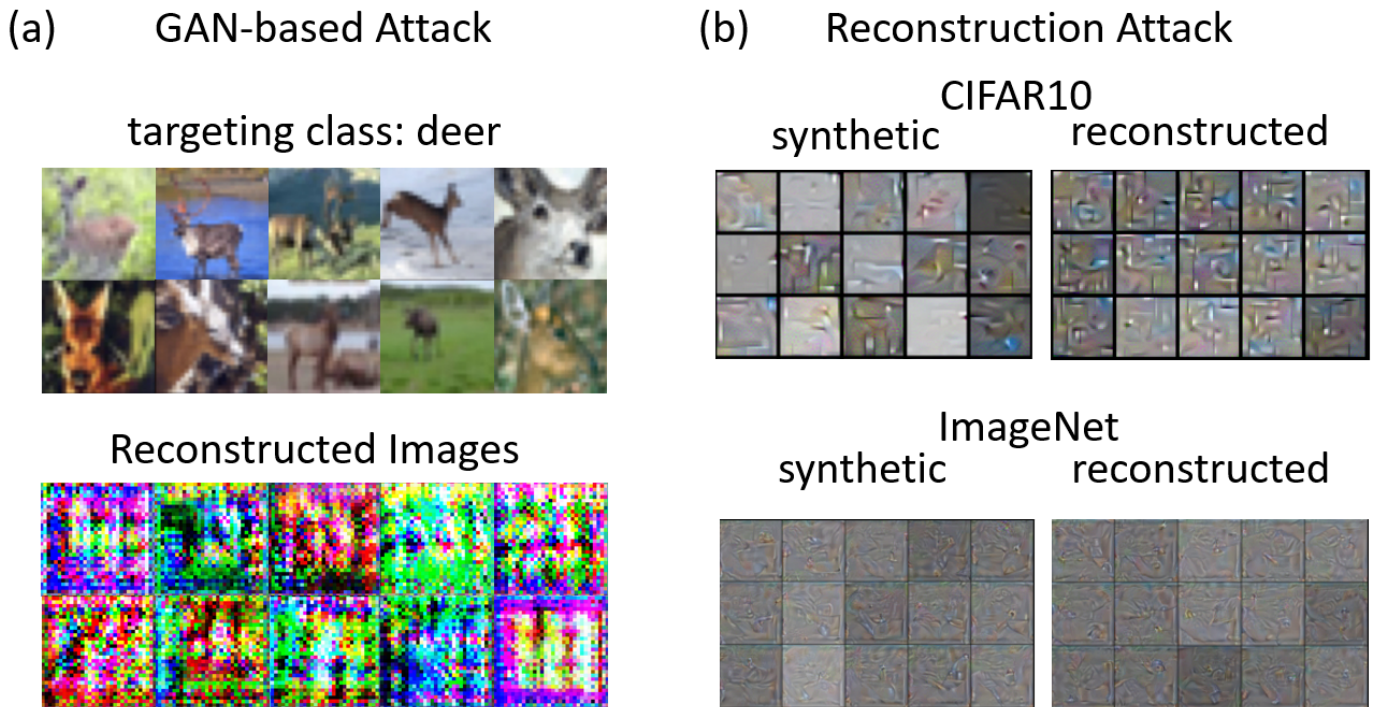


Fig. 4. (a) GAN-based attack targeting the deer class from CIFAR10, (b) Synthetic Images and Reconstructed Images, when the attacker tries to invert our algorithm with Reconstruction Attack.

TABLE VI

EVALUATION USING IMAGE QUALITY METRICS ON CIFAR10 AND IMAGENET FOR THE RECONSTRUCTION ATTACK. HIGHER MSE, SSIM AND HAARPSI DENOTE HIGHER DISSIMILARITY AMONG DIFFERENT SETS OF IMAGES.

Dataset	Metric	Original/Reconstructed Images	Synthetic/Reconstructed Images
CIFAR10	MSE	2.9043	2.1400
	SSIM	0.0081	0.0083
	HaarPSI	0.2641	0.4744
ImageNet	MSE	3.1834	2.8252
	SSIM	0.0006	0.0012
	HaarPSI	0.1868	0.4026

has access to the synthetic images but not the original images. Fig. 4 (a) illustrates an example of such attack on target class - deer. Here, the attacker aims to reconstruct images of the deer class from CIFAR10. The reconstructed images after performing the GAN-based attack is shown in the second row of Fig. 4 (a). The result shows that the attacker is neither able to reconstruct the original images nor reveal distinct image features.

The evaluation of our method against known attacks reveals that the synthetic images do not leak visual information about the original images. The attacker can at most reconstruct the synthetic images but not the source original images. Moreover, it is important to verify if the attacker, following a process similar to our algorithm, is able to obtain the original images. In our proposed method, we pre-trained network on the original images and using its BN statistics we generated the desired synthetic images. Now, we ask whether training a network on synthetic images and then using the BN statistics, can an attacker synthesize images that look visually similar to the original images. We denote this attack as **Reconstruction**

Attack and perform experiment using a ResNet20 network on CIFAR10 and a ResNet18 network on ImageNet. Figure 4 (b) illustrates our synthetic images versus the images that the attacker is able to synthesize with this attack. We observe that, for both CIFAR10 and ImageNet, the reconstructed images are highly distorted compared to the original images and the synthetic images. The synthetic image generation inherently distorts the images. In the attempt to generate new synthetic images from a network trained on synthetic images, this adds more distortion on the images. Tables VI compares the Image Quality Metrics between the original and the reconstructed images and the synthetic and reconstructed images for both CIFAR10 and ImageNet. From the image quality metrics, we observe that the synthetic and the reconstructed images have a higher similarity compared to the the original and the reconstructed images which are highly dissimilar. Thus, visual-privacy of our synthetic images is protected against such attacks.

V. CONCLUSIONS

In this paper, we present a method for generating synthetic images that can be used for privacy-preserving ML applications. Our method makes use of the BN statistics of the network pre-trained on the original images and optimizes random noise to generate synthetic data that, when fed into the network, have a layer-wise statistical distribution that closely matches the original images. We evaluate our method on image classification datasets including CIFAR10 and ImageNet. Our experiments show that synthetic images maintain data-utility. In other words, network performs equally well when synthetic images are used instead of the original images. Additionally, we find that data-utility of the synthetic images transfers across different network architectures. Moreover, with various image quality metrics (MSE, SSIM, HaarPSI) we show that the synthetic images are visually dissimilar to the original source images. Despite such visual dissimilarity, synthetic images can potentially leak visual information about the original images. Therefore, we further assessed our method against privacy-leakage attack such as gradient matching attack, model memorization attack, and GAN-based attack. Our analyses show that in all these cases, the attacker can, at most, reveal visual information about the synthetic images, but can not obtain the original images. Overall, the results and analyses provide strong evidences in favor of the effectiveness of our synthetic datasets generation method for privacy-preserving ML applications.

APPENDIX

We hereby provide more details for the privacy-leakage attacks in Section IV-C: Gradient Matching Attack [25] (Algorithm 2) and GAN-based Attack (Algorithm 3).

Algorithm 2 Gradients Matching Attack

- 1: **Require:** The function $F(x; W)$ is a neural network with L layers trained on the given images (in our case synthetic images), we define $W_l \in \mathbb{R}^{m_l \times m_{l-1}}$ to be the weight matrix in l -th layer for $l = 1, \dots, L$, and $m_l = d_i$ and $m_l = d_o$, $W = W_1, W_2, \dots, W_L$ denotes the weights over all layers
 - 2: Let (x_0, y_0) denote a (image, label) pair \triangleright in our case, x_0 is synthetic image
 - 3: Let $\mathcal{L} : \mathbb{R}^{d_o \times d_o} \rightarrow \mathbb{R}$ denote the loss function
 - 4: Let $g(x, y) = \nabla \mathcal{L}(F(x; W), y)$ denote the gradients of loss function, and $\hat{g} = g(x, y)|_{x=x_0, y=y_0}$ is the gradients computed on x_0 with label y_0
 - 5: **Procedure:** Input Recovery From Gradients()
 - 6: $x^{(1)} \leftarrow \mathcal{N}(0, 1), y^{(1)} \leftarrow \mathcal{N}(0, 1)$
 - 7: **for** $t = 1 \rightarrow T$ **do**
 - 8: Let $D_g(x, y) = \|g(x, y) - \hat{g}\|_2^2$
 - 9: $x^{(t+1)} \leftarrow x^{(t)} - \eta \cdot \nabla_x D_g(x, y)|_{x=x^{(t)}}$
 - 10: $y^{(t+1)} \leftarrow y^{(t)} - \eta \cdot \nabla_y D_g(x, y)|_{y=y^{(t)}}$
 - 11: **end for**
 - 12: **Return** $x^{(T+1)}, y^{(T+1)}$
 - 13: **End Procedure**
-

Algorithm 3 GAN-based Attack

- 1: **Require:** Synthetic Images, neural network (NN) to be trained on the synthetic images, GAN consisting of a generator (G) and a discriminator (D), targeting class a
 - 2: **for** epoch = 1 $\rightarrow T$ **do**
 - 3: Run SGD for NN on Synthetic Images and update NN
 - 4: **Adversary:**
 - 5: Create a replica of NN as D
 - 6: Run G on D targeting class a
 - 7: Update G based on the answer from D
 - 8: Get n -samples of class a generated by G
 - 9: Assign label c (fake label) to generated samples of class a
 - 10: Merge the generated data with the Synthetic Images
 - 11: **end for**
 - 12: **Return** the images generated from G on targeting class a
-

REFERENCES

- [1] <https://azure.microsoft.com/en-us/services/machine-learning-studio/>.
- [2] <https://cloud.google.com/ml-engine/docs/technical-overview>.
- [3] <https://aws.amazon.com/sagemaker/>.
- [4] T. Zhang, Z. He, and R. B. Lee, "Privacy-preserving machine learning through data obfuscation," *arXiv preprint arXiv:1807.01860*, 2018.
- [5] A. Triastcyn and B. Faltings, "Generating artificial data for private deep learning," *arXiv preprint arXiv:1803.03148*, 2018.
- [6] R. Bost, R. A. Popa, S. Tu, and S. Goldwasser, "Machine learning classification over encrypted data," *Cryptology ePrint Archive*, 2014.
- [7] W. Sirichotedumrong, T. Maekawa, Y. Kinoshita, and H. Kiya, "Privacy-preserving deep neural networks with pixel-based image encryption considering data augmentation in the encrypted domain," in *2019 IEEE International Conference on Image Processing (ICIP)*. IEEE, 2019, pp. 674–678.
- [8] Y. Aono, T. Hayashi, L. Trieu Phong, and L. Wang, "Scalable and secure logistic regression via homomorphic encryption," in *Proceedings of the Sixth ACM Conference on Data and Application Security and Privacy*, 2016, pp. 142–144.
- [9] C. Bonte and F. Vercauteren, "Privacy-preserving logistic regression training," *BMC medical genomics*, vol. 11, no. 4, pp. 13–21, 2018.
- [10] J. L. Crawford, C. Gentry, S. Halevi, D. Platt, and V. Shoup, "Doing real work with fhe: the case of logistic regression," in *Proceedings of the 6th Workshop on Encrypted Computing & Applied Homomorphic Cryptography*, 2018, pp. 1–12.
- [11] M. Kim, Y. Song, S. Wang, Y. Xia, X. Jiang *et al.*, "Secure logistic regression based on homomorphic encryption: Design and evaluation," *JMIR medical informatics*, vol. 6, no. 2, p. e8805, 2018.
- [12] T. Graepel, K. Lauter, and M. Naehrig, "MI confidential: Machine learning on encrypted data," in *International Conference on Information Security and Cryptology*. Springer, 2012, pp. 1–21.
- [13] K. Nandakumar, N. Ratha, S. Pankanti, and S. Halevi, "Towards deep neural network training on encrypted data," in *Proceedings of the IEEE/CVF Conference on Computer Vision and Pattern Recognition Workshops*, 2019, pp. 0–0.
- [14] B. Jayaraman and D. Evans, "Evaluating differentially private machine learning in practice," in *28th USENIX Security Symposium (USENIX Security 19)*, 2019, pp. 1895–1912.
- [15] C. Neustaedter, S. Greenberg, and M. Boyle, "Blur filtration fails to preserve privacy for home-based video conferencing," *ACM Transactions on Computer-Human Interaction (TOCHI)*, vol. 13, no. 1, pp. 1–36, 2006.
- [16] H. Inoue, "Data augmentation by pairing samples for images classification," *arXiv preprint arXiv:1801.02929*, 2018.
- [17] H. Zhang, M. Cisse, Y. N. Dauphin, and D. Lopez-Paz, "mixup: Beyond empirical risk minimization," *arXiv preprint arXiv:1710.09412*, 2017.
- [18] M. Raynal, R. Achanta, and M. Humbert, "Image obfuscation for privacy-preserving machine learning," *arXiv preprint arXiv:2010.10139*, 2020.

- [19] Y. Cai, Z. Yao, Z. Dong, A. Gholami, M. W. Mahoney, and K. Keutzer, "Zero: A novel zero shot quantization framework," in *Proceedings of the IEEE/CVF Conference on Computer Vision and Pattern Recognition*, 2020, pp. 13 169–13 178.
- [20] A. Krizhevsky, G. Hinton *et al.*, "Learning multiple layers of features from tiny images," 2009.
- [21] J. Deng, W. Dong, R. Socher, L.-J. Li, K. Li, and L. Fei-Fei, "Imagenet: A large-scale hierarchical image database," in *2009 IEEE conference on computer vision and pattern recognition*. Ieee, 2009, pp. 248–255.
- [22] C. Rafael, "Gonzalez, and richard e. woods," *Digital image processing*, p. 793, 1992.
- [23] Z. Wang, A. C. Bovik, H. R. Sheikh, and E. P. Simoncelli, "Image quality assessment: from error visibility to structural similarity," *IEEE transactions on image processing*, vol. 13, no. 4, pp. 600–612, 2004.
- [24] R. Reisenhofer, S. Bosse, G. Kutyniok, and T. Wiegand, "A haar wavelet-based perceptual similarity index for image quality assessment," *Signal Processing: Image Communication*, vol. 61, pp. 33–43, 2018.
- [25] L. Zhu, Z. Liu, and S. Han, "Deep leakage from gradients," in *Advances in Neural Information Processing Systems*, 2019.
- [26] C. Song, T. Ristenpart, and V. Shmatikov, "Machine learning models that remember too much," in *Proceedings of the 2017 ACM SIGSAC Conference on computer and communications security*, 2017, pp. 587–601.
- [27] B. Hitaj, G. Ateniese, and F. Perez-Cruz, "Deep models under the gan: information leakage from collaborative deep learning," in *Proceedings of the 2017 ACM SIGSAC conference on computer and communications security*, 2017, pp. 603–618.
- [28] Z. Huang, R. Hu, Y. Guo, E. Chan-Tin, and Y. Gong, "Dp-admm: Admm-based distributed learning with differential privacy," *IEEE Transactions on Information Forensics and Security*, vol. 15, pp. 1002–1012, 2019.
- [29] N. Papernot, S. Song, I. Mironov, A. Raghunathan, K. Talwar, and Ú. Erlingsson, "Scalable private learning with pate," *arXiv preprint arXiv:1802.08908*, 2018.
- [30] N. Papernot, M. Abadi, U. Erlingsson, I. Goodfellow, and K. Talwar, "Semi-supervised knowledge transfer for deep learning from private training data," *arXiv preprint arXiv:1610.05755*, 2016.
- [31] M. Fredrikson, E. Lantz, S. Jha, S. Lin, D. Page, and T. Ristenpart, "Privacy in pharmacogenetics: An {End-to-End} case study of personalized warfarin dosing," in *23rd USENIX Security Symposium (USENIX Security 14)*, 2014, pp. 17–32.
- [32] M. Abadi, A. Chu, I. Goodfellow, H. B. McMahan, I. Mironov, K. Talwar, and L. Zhang, "Deep learning with differential privacy," in *Proceedings of the 2016 ACM SIGSAC conference on computer and communications security*, 2016, pp. 308–318.
- [33] L. Fan, "Differential privacy for image publication," in *Theory and Practice of Differential Privacy (TPDP) Workshop*, vol. 1, no. 2, 2019, p. 6.
- [34] K. Lee, H. Kim, K. Lee, C. Suh, and K. Ramchandran, "Synthesizing differentially private datasets using random mixing," in *2019 IEEE International Symposium on Information Theory (ISIT)*. IEEE, 2019, pp. 542–546.
- [35] L. Fan, "Practical image obfuscation with provable privacy," in *2019 IEEE International Conference on Multimedia and Expo (ICME)*. IEEE, 2019, pp. 784–789.
- [36] T. Li and M. S. Choi, "Deepblur: A simple and effective method for natural image obfuscation," *arXiv preprint arXiv:2104.02655*, vol. 1, 2021.
- [37] A. Poller, M. Steinebach, and H. Liu, "Robust image obfuscation for privacy protection in web 2.0 applications," in *Media Watermarking, Security, and Forensics 2012*, vol. 8303. International Society for Optics and Photonics, 2012, p. 830304.
- [38] M. Fredrikson, S. Jha, and T. Ristenpart, "Model inversion attacks that exploit confidence information and basic countermeasures," in *Proceedings of the 22nd ACM SIGSAC conference on computer and communications security*, 2015, pp. 1322–1333.
- [39] G. Ateniese, L. V. Mancini, A. Spognardi, A. Villani, D. Vitali, and G. Felici, "Hacking smart machines with smarter ones: How to extract meaningful data from machine learning classifiers," *International Journal of Security and Networks*, vol. 10, no. 3, pp. 137–150, 2015.
- [40] R. Shokri, M. Stronati, C. Song, and V. Shmatikov, "Membership inference attacks against machine learning models," in *2017 IEEE symposium on security and privacy (SP)*. IEEE, 2017, pp. 3–18.
- [41] I. Garg, M. Nagaraj, and K. Roy, "Tofu: Towards obfuscated federated updates by encoding weight updates into gradients from proxy data," *arXiv preprint arXiv:2201.08494*, 2022.
- [42] M. Alkhalaiwi, W. Boulila, J. Ahmad, A. Koubaa, and M. Driss, "An efficient approach based on privacy-preserving deep learning for satellite image classification," *Remote Sensing*, vol. 13, no. 11, p. 2221, 2021.
- [43] B. Liu, M. Ding, S. Shaham, W. Rahayu, F. Farokhi, and Z. Lin, "When machine learning meets privacy: A survey and outlook," *ACM Computing Surveys (CSUR)*, vol. 54, no. 2, pp. 1–36, 2021.
- [44] Y. Zhong, M. Lin, G. Nan, J. Liu, B. Zhang, Y. Tian, and R. Ji, "Intraq: Learning synthetic images with intra-class heterogeneity for zero-shot network quantization," *arXiv preprint arXiv:2111.09136*, 2021.
- [45] M. Haroush, I. Hubara, E. Hoffer, and D. Soudry, "The knowledge within: Methods for data-free model compression," in *Proceedings of the IEEE/CVF Conference on Computer Vision and Pattern Recognition*, 2020, pp. 8494–8502.
- [46] B. Li, K. Huang, S. Chen, D. Xiong, H. Jiang, and L. Claesen, "DFQF: Data free quantization-aware fine-tuning," in *Asian Conference on Machine Learning*. PMLR, 2020, pp. 289–304.
- [47] A. Mordvintsev, C. Olah, and M. Tyka, "Inceptionism: Going deeper into neural networks," 2015.
- [48] J. Smith, Y.-C. Hsu, J. Balloch, Y. Shen, H. Jin, and Z. Kira, "Always be dreaming: A new approach for data-free class-incremental learning," in *Proceedings of the IEEE/CVF International Conference on Computer Vision*, 2021, pp. 9374–9384.
- [49] H. Chen, Y. Wang, C. Xu, Z. Yang, C. Liu, B. Shi, C. Xu, C. Xu, and Q. Tian, "Data-free learning of student networks," in *Proceedings of the IEEE/CVF International Conference on Computer Vision*, 2019, pp. 3514–3522.
- [50] H. Yin, P. Molchanov, J. M. Alvarez, Z. Li, A. Mallya, D. Hoiem, N. K. Jha, and J. Kautz, "Dreaming to distill: Data-free knowledge transfer via deepinversion," in *Proceedings of the IEEE/CVF Conference on Computer Vision and Pattern Recognition*, 2020, pp. 8715–8724.
- [51] X. He, J. Lu, W. Xu, Q. Hu, P. Wang, and J. Cheng, "Generative zero-shot network quantization," in *Proceedings of the IEEE/CVF Conference on Computer Vision and Pattern Recognition*, 2021, pp. 3000–3011.
- [52] K. He, X. Zhang, S. Ren, and J. Sun, "Deep residual learning for image recognition," in *Proceedings of the IEEE conference on computer vision and pattern recognition*, 2016, pp. 770–778.
- [53] K. Simonyan and A. Zisserman, "Very deep convolutional networks for large-scale image recognition," *arXiv preprint arXiv:1409.1556*, 2014.
- [54] M. Sandler, A. Howard, M. Zhu, A. Zhmoginov, and L.-C. Chen, "Mobilenetv2: Inverted residuals and linear bottlenecks," in *Proceedings of the IEEE conference on computer vision and pattern recognition*, 2018, pp. 4510–4520.
- [55] A. Paszke, S. Gross, F. Massa, A. Lerer, J. Bradbury, G. Chanan, T. Killeen, Z. Lin, N. Gimelshein, L. Antiga, A. Desmaison, A. Kopf, E. Yang, Z. DeVito, M. Raison, A. Tejani, S. Chilamkurthy, B. Steiner, L. Fang, J. Bai, and S. Chintala, "Pytorch: An imperative style, high-performance deep learning library," in *Advances in Neural Information Processing Systems 32*, 2019, pp. 8024–8035.
- [56] J. Kiefer and J. Wolfowitz, "Stochastic estimation of the maximum of a regression function," *The Annals of Mathematical Statistics*, pp. 462–466, 1952.
- [57] D. P. Kingma and J. Ba, "Adam: A method for stochastic optimization," *arXiv preprint arXiv:1412.6980*, 2014.
- [58] "Computer vision models on pytorch." [Online]. Available: <https://pytorch.org/project/pytorchcv/>
- [59] G. Huang, Z. Liu, L. Van Der Maaten, and K. Q. Weinberger, "Densely connected convolutional networks," in *Proceedings of the IEEE conference on computer vision and pattern recognition*, 2017, pp. 4700–4708.



Efstathia Soufleri (Graduate Student Member, IEEE) received her bachelor's degree from the Department of Mathematics at the National and Kapodistrian University of Athens, Greece, in 2016. She was awarded a scholarship from the Greek National Foundation for academic excellence during her studies in 2016. She received her master's degree with honors in Computer Science from the University of Thessaly, Greece, in 2017.

She is currently a research assistant at Nanoelectronics Research Laboratory (NRL). She is pursuing her Ph.D. in Electrical and Computer Engineering at Purdue University, West Lafayette, Indiana, USA under the guidance of Prof. Kaushik Roy. Her primary research interests lie in the field of Neural Network Compression and Neuro-inspired Algorithms for Efficient Learning.



Gobinda Saha received the B.Sc. and M.Sc. degrees in electrical and electronic engineering from the Bangladesh University of Engineering and Technology, Dhaka, Bangladesh, in 2013 and 2015, respectively. He is currently pursuing the Ph.D. degree with Purdue University, under the guidance of Prof. Kaushik Roy. In Summer 2019, he worked as a Research Intern with the Memory Solution Team, Global Foundries, Santa Clara, CA, USA. His primary research interests include efficient algorithm design for continual learning, representation learning,

and meta-learning.



Kaushik Roy (Fellow, IEEE) received the B.Tech. degree in electronics and electrical communications engineering from IIT Kharagpur, Kharagpur, India, and the Ph.D. degree from the Electrical and Computer Engineering Department, University of Illinois at Urbana-Champaign, in 1990.

He was with the Semiconductor Process and Design Center of Texas Instruments, Dallas, where he worked on FPGA architecture development and low-power circuit design. He joined the Electrical and Computer Engineering Faculty, Purdue University, West Lafayette, IN, USA, in 1993, where he is currently the Edward G. Tiedemann Jr. Distinguished Professor. He is the Director of the Center for Brain-Inspired Computing (C-BRIC) funded by SRC/DARPA. He has published more than 700 articles in refereed journals and conferences, holds 25 patents, supervised 85 Ph.D. dissertations, and is co-author of two books on Low Power CMOS VLSI Design (John Wiley & McGraw Hill). His research interests include neuromorphic and emerging computing models, neuromimetic devices, spintronics, device-circuitalgorithm co-design for nano-scale silicon, non-silicon technologies, and low-power electronics. He received the National Science Foundation Career Development Award, in 1995, the IBM Faculty Partnership Award, the ATT/Lucent Foundation Award, the 2005 SRC Technical Excellence Award, the SRC Inventors Award, the Purdue College of Engineering Research Excellence Award, the Humboldt Research Award, in 2010, the 2010 IEEE Circuits and Systems Society Technical Achievement Award (Charles Desoer Award), the Distinguished Alumnus Award from IIT Kharagpur, the Fulbright-Nehru Distinguished Chair, the DoD Vannevar Bush Faculty Fellow, from 2014 to 2019, the Semiconductor Research Corporation Aristotle Award, in 2015, the 2020 Arden Bement Jr. Award, the Highest Research Award given by Purdue University in pure and applied science and engineering, and the Best Paper Awards at 1997 International Test Conference, the IEEE 2000 International Symposium on Quality of IC Design, the 2003 IEEE Latin American Test Workshop, the 2003 IEEE Nano, the 2004 IEEE International Conference on Computer Design, the 2006 IEEE/ACM International Symposium on Low Power Electronics and Design, and the 2005 IEEE Circuits and System Society Outstanding Young Author Award (Chris Kim), the 2006 IEEE TRANSACTIONS ON VLSI SYSTEMS Best Paper Award, the 2012 ACM/IEEE International Symposium on Low Power Electronics and Design Best Paper Award, and the 2013 IEEE TRANSACTIONS ON VLSI Best Paper Award. He was a Purdue University Faculty Scholar from 1998 to 2003. He was a Research Visionary Board Member of Motorola Labs, in 2002 and held the M. Gandhi Distinguished Visiting Faculty with IIT Bombay and the Global Foundries Visiting Chair with the National University of Singapore. He has been in the editorial board of IEEE Design and Test, the IEEE TRANSACTIONS ON CIRCUITS AND SYSTEMS, the IEEE TRANSACTIONS ON VLSI SYSTEMS, and the IEEE TRANSACTIONS ON ELECTRON DEVICES. He was a Guest Editor for Special Issue on Low-Power VLSI in IEEE Design and Test, in 1994, the IEEE TRANSACTIONS ON VLSI SYSTEMS, in June 2000, the IEE Proceedings-Computers and Digital Techniques, in July 2002, and the IEEE JOURNAL ON EMERGING AND SELECTED TOPICS IN CIRCUITS AND SYSTEMS, in 2011.

He was with the Semiconductor Process and Design Center of Texas Instruments, Dallas, where he worked on FPGA architecture development and low-power circuit design. He joined the Electrical and Computer Engineering Faculty, Purdue University, West Lafayette, IN, USA, in 1993, where he is currently the Edward G. Tiedemann Jr. Distinguished Professor. He is the Director of the Center for Brain-Inspired Computing (C-BRIC) funded by SRC/DARPA. He has published more than 700 articles in refereed journals and conferences, holds 25 patents, supervised 85 Ph.D. dissertations, and is co-author of two books on Low Power CMOS VLSI Design (John Wiley & McGraw Hill). His research interests include neuromorphic and emerging computing models, neuromimetic devices, spintronics, device-circuitalgorithm co-design for nano-scale silicon, non-silicon technologies, and low-power electronics. He received the National Science Foundation Career Development Award, in 1995, the IBM Faculty Partnership Award, the ATT/Lucent Foundation Award, the 2005 SRC Technical Excellence Award, the SRC Inventors Award, the Purdue College of Engineering Research Excellence Award, the Humboldt Research Award, in 2010, the 2010 IEEE Circuits and Systems Society Technical Achievement Award (Charles Desoer Award), the Distinguished Alumnus Award from IIT Kharagpur, the Fulbright-Nehru Distinguished Chair, the DoD Vannevar Bush Faculty Fellow, from 2014 to 2019, the Semiconductor Research Corporation Aristotle Award, in 2015, the 2020 Arden Bement Jr. Award, the Highest Research Award given by Purdue University in pure and applied science and engineering, and the Best Paper Awards at 1997 International Test Conference, the IEEE 2000 International Symposium on Quality of IC Design, the 2003 IEEE Latin American Test Workshop, the 2003 IEEE Nano, the 2004 IEEE International Conference on Computer Design, the 2006 IEEE/ACM International Symposium on Low Power Electronics and Design, and the 2005 IEEE Circuits and System Society Outstanding Young Author Award (Chris Kim), the 2006 IEEE TRANSACTIONS ON VLSI SYSTEMS Best Paper Award, the 2012 ACM/IEEE International Symposium on Low Power Electronics and Design Best Paper Award, and the 2013 IEEE TRANSACTIONS ON VLSI Best Paper Award. He was a Purdue University Faculty Scholar from 1998 to 2003. He was a Research Visionary Board Member of Motorola Labs, in 2002 and held the M. Gandhi Distinguished Visiting Faculty with IIT Bombay and the Global Foundries Visiting Chair with the National University of Singapore. He has been in the editorial board of IEEE Design and Test, the IEEE TRANSACTIONS ON CIRCUITS AND SYSTEMS, the IEEE TRANSACTIONS ON VLSI SYSTEMS, and the IEEE TRANSACTIONS ON ELECTRON DEVICES. He was a Guest Editor for Special Issue on Low-Power VLSI in IEEE Design and Test, in 1994, the IEEE TRANSACTIONS ON VLSI SYSTEMS, in June 2000, the IEE Proceedings-Computers and Digital Techniques, in July 2002, and the IEEE JOURNAL ON EMERGING AND SELECTED TOPICS IN CIRCUITS AND SYSTEMS, in 2011.